

PACS: 52.80.-s, 51.50.+v, 52.80.Tn, 52.90.+z, 52.80.Mg, 79.60.Jv

ISSN 1729-4428 (Print)  
ISSN 2309-8589 (Online)

O.K. Shuaibov, R.V. Hrytsak, O.Y. Minya, A.O. Malinina, I.V. Shevera, Yu.Yu. Bilak,  
Z.T. Homoki

## Conditions for pulsed gas-discharge synthesis of thin tungsten oxide films from a plasma mixture of air with tungsten vapors

*Uzhhorod National University, Uzhhorod, Ukraine, [alexander.shuaibov@uzhnu.edu.ua](mailto:alexander.shuaibov@uzhnu.edu.ua)*

Characteristics of high-voltage nanosecond discharge in gas-vapor mixtures "Air – W" at air pressures  $p = 101.13; 13.3$  kPa are provided. The discharge was ignited between tungsten electrodes. Formation of tungsten oxide clusters in the plasma occurred during the introduction of tungsten vapors into the discharge gap via an electron mechanism, creating conditions for the synthesis of thin tungsten oxide ( $WO_3$ ) films deposited on a glass substrate.

The optical properties of the discharge from the central region of a 2 mm-wide gap were investigated. The main components responsible for excitation in the plasma of a tungsten-based vapor-gas mixture with air were identified. Examination of the Raman spectra of laser-scattered radiation by the experimentally synthesized thin films revealed them to be island-like films of tungsten oxide ( $WO_3$ ).

**Keywords:** overvoltage nanosecond discharge, tungsten, air, thin films, radiation spectrum, plasma.

*Received 29 April 2024; Accepted 10 October 2024.*

### Introduction

When igniting a high-voltage nanosecond discharge (HVND) in gases at atmospheric pressure between metal electrodes at a small electrode separation distance ( $d = 1-3$  mm), material dispersion from the electrodes occurs [1], even for refractory metals such as tungsten [2]. For this type of discharge (under significant overvoltage in the discharge gap), the appearance of electrons [2,3] and "runaway electrons" capable of transitioning into a continuous acceleration mode is characteristic [4]. Under these discharge conditions, the existence of "runaway electrons" and their accompanying X-ray emission serve as a pre-ionization system in the discharge gap. This leads to the formation of a uniform discharge at atmospheric pressure, which can be utilized for depositing thin films from the dispersed material of the electrodes and the corresponding gas environment [5].

Tungsten and molybdenum oxides ( $WO_3$ ,  $MoO_3$ ) are used for reversible color change in thin film oxidation-reduction reactions when an external voltage is applied to them (electrochromism phenomenon) [6]. The synthesis

of thin films of tungsten and molybdenum oxides is largely carried out by chemical methods or by the explosion of thin wires. In [7], oxides were synthesized in the form of micro- and nanoscale powders through the electric explosion method of a tungsten conductor in air. Analysis of the explosion products showed that the sole product of the breakdown of the tungsten conductor was a mixture of powders  $WO_3 + W_2O_7$ , with the predominant formation of tungsten anhydride –  $WO_3$ .

In [8], the results of the chemical synthesis of tungsten oxide ( $WO_3$ ) nanoplates on fluorine-doped tin oxide glass substrates using hydrothermal techniques are presented. The synthesis of tungsten oxide films with a thickness of 36-180 nm by microwave methods was reported in [9], where their transmittance spectra in the visible and near-infrared regions were also provided, both in colored and colorless states. The results of synthesizing tungsten oxide films with a thickness of 42-131 nm by reactive sputtering are presented in [10], where it was found that after annealing at 500°C, they transformed into stable crystalline structures.

Currently, there are no results available for the

synthesis of thin tungsten oxide films deposited from the plasma of a gas-vapor mixture "Air – W" (utilizing the electron erosion mechanism of tungsten electrodes). Such a technology for synthesizing thin tungsten oxide films does not require the use of vacuum techniques or expensive buffer gases. It's also worth noting that when depositing tungsten oxide films onto tungsten, its microhardness increases.

The article presents the results of investigating the characteristics of a high-voltage nanosecond discharge between tungsten electrodes in air, which can be applied for synthesizing thin tungsten oxide films.

## I. Technique and conditions of the experiment

The investigation of HVND characteristics in air was conducted using an experimental setup, the schematic and main specifications of which are provided in [1]. The distance between the electrodes was set to  $d = 2$  mm. The electrodes were made of tungsten in the form of rods with a diameter of 5 mm and a length of 50 mm, with rounded radii of the working part measuring 3 mm. They were installed in a discharge chamber made of dielectric material.

To initiate the discharge on the electrodes, bipolar high-voltage pulses lasting 100-150 ns were used, with amplitudes ranging from  $\pm 20$  to  $\pm 40$  kV. The frequency of the voltage pulse sequence was in the range of 80 to 1000 Hz. The air pressure was maintained at 101.2; 13.3 kPa.

The overvoltage discharge created conditions conducive to the formation of a beam of "runaway electrons" with high energy and X-ray radiation [4].

A forevacuum pump was used to evacuate the chamber to a residual pressure of 5-10 Pa. After evacuation, air was introduced into the chamber at a pressure of 13.3 kPa.

## II. Discharge characteristics

At a distance of  $d = 2$  mm between the electrodes and atmospheric air pressure ( $p = 101$  kPa), the HVND appeared as an intense central region with a diameter of

approximately 2-3 mm, surrounded by a series of less intense plasma jets emanating from the central portion.

Figure 1 shows the oscillograms of current, voltage, and pulsed power for the discharge between tungsten electrodes at different air pressures and with a voltage magnitude on the anode of the high-voltage pulse modulator triode of 13 kV.

The oscillograms of current and voltage displayed decaying oscillations with a duration of approximately 80-100 ns, arising due to mismatch between the output impedance of the high-voltage pulse modulator and the load impedance. The total duration of voltage and discharge current oscillations was 450-500 ns.

For HVND at atmospheric air pressure, the amplitude of positive polarity voltage on the electrodes reached approximately 30 kV at the initial stage of the discharge, with a current of approximately 100 A. The maximum pulsed power of the discharge reached 3 MW at  $t = 30$  ns, with an energy contribution to the plasma of 312.6 mJ.

When reducing the air pressure to 13.3 kPa, the maximum amplitude of positive polarity voltage decreased to 12 kV, and the peak half-wave current reached 125 A. The pulsed power of the discharge reached 1.25 MW at  $t = 90$  ns. The energy contribution to the plasma based on atmospheric air pressure was 176.9 mJ.

For the control experiment conducted with a discharge on a mixture of tungsten vapors with oxygen as the buffer gas at a pressure of  $p = 103$  kPa, the appearance of the voltage and current oscillograms remained unchanged, but the energy characteristics of the HVND decreased: the pulsed power was 2.4 MW, and the energy contribution to the plasma per pulse was 245.4 mJ. This could be attributed to the different potentials of stepwise ionization of oxygen and nitrogen molecules. A similar pattern was observed for discharges with buffer gases such as Ne and Kr: in the case of heavy inert gas, the energy characteristics of the HVND prevailed over those of the corresponding light inert gas (Ne) with a higher potential of stepwise ionization. For nanosecond discharges at elevated pressure, the prevalence of stepwise ionization processes over direct ionization is characteristic [11].

The spectrum of HVND radiation in the mixture of air with tungsten vapors is shown in Figure 2, and the results of identifying the spectral lines of atoms and ions are presented in Table 1. The decoding of plasma emission spectra was carried out using handbooks [12,13].

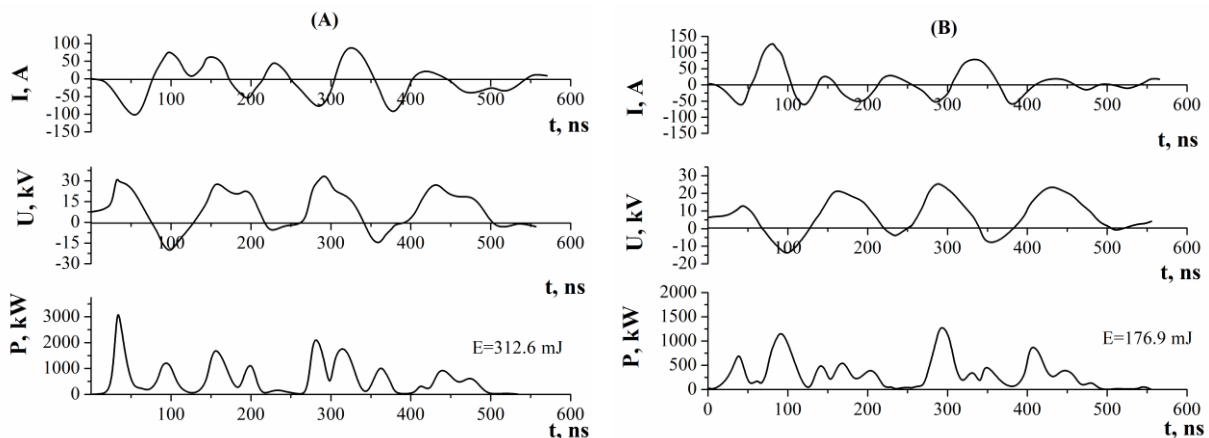
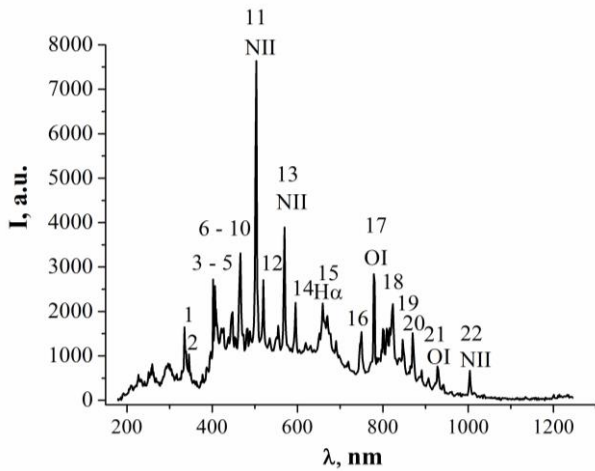


Fig. 1. Oscillograms of current, voltage, and pulsed power of the discharge between tungsten electrodes at air pressures of 101 (A) and 13.3 (B) kPa.



**Fig.2.** Spectrum of HVND plasma radiation between tungsten electrodes at air pressure of 101 kPa ( $f = 1000$  Hz,  $d = 2$  mm).

For plasma formed as a result of non-overvoltage nanosecond discharges in atmospheric air pressure (with an electrode spacing of 10 mm), the ultraviolet emission spectrum was mainly determined by bands of the second positive system of  $N_2$  molecules, carbon nitride bands, OH radical, NO, as well as lines of singly charged ions and atoms of oxygen and nitrogen [14]. In our case, for the spectra of HVND plasma emission, the molecular component of plasma emission was absent, which was due to the rapid ionization of molecules in a strong electric field.

A similar pattern was observed for the plasma of the gas-vapor mixture "O<sub>2</sub> – W" [15]. In the emission spectra of HVND based on the gas-vapor mixture "oxygen-

tungsten," predominantly spectral lines of O I, O II, and O III were observed.

The spectral lines of atomic and ion emission from HVND plasma in gas mixtures of air with tungsten vapors were observed against the background of continuous plasma radiation. The most pronounced continuum in HVND radiation was observed in the spectral range of 400-500 nm.

The significant intensity of radiation on the transitions of nitrogen ion spectral lines above the radiation of nitrogen atoms may be due to the recombination mechanism populating the upper energy levels of atomic nitrogen ions in the overvoltage nanosecond discharge [14]. The energies of the upper energy levels for the spectral lines of N II are in the range from 21 to 26 eV. This indicates a high electron temperature in the investigated plasma, as the presence of doubly charged atomic nitrogen ions is required for the recombination of ions with plasma electrons.

### III. Raman scattering spectra

A detailed method of synthesis and sputtering of thin films, which were synthesized from electrode erosion products, is given in [16]. The films were analyzed using all three available wavelengths of diode lasers (532, 633, and 785 nm) using the Renishaw InVia confocal Raman microscope (UK) equipped with a spectrometer for Raman light scattering. The diameter of the laser beam was 1  $\mu$ m.

The Raman scattering spectra of laser radiation from thin films deposited from the plasma of the vapor-gas mixture "Air – W" at atmospheric air pressure are shown in Figure 3. The spectra were recorded from islands with sizes ranging from 3 to 10  $\mu$ m, consisting of a compound

**Table 1.** Results of identification of plasma emission spectra of HVND between tungsten electrodes at air pressure of 101 kPa ( $d = 2$  mm;  $f = 1000$  Hz)

№	$\lambda_{\text{tab}}, \text{nm}$	$I_{\text{exp}} \text{ a. u.}$	Object	$E_{\text{low}}, \text{eV}$	$E_{\text{up}}, \text{eV}$	Term <sub>low</sub>	Term <sub>up</sub>
1	332.97	1646	N II	17.87	21.59	$2s^2p^3 \ ^1D_2$	$2s^2p^3p \ ^1D_2$
2	343.71	1031	N II	18.49	22.10	$2s^2p^3s \ ^1P_1$	$2s^2p^3p \ ^1S_0$
3	395.53	1089	W I	2.43	5.57	$5d^5(^4G)6s \ ^5G_6$	$5d^3(^4F)6s(^5F)6p \ ^6G_6$
4	400.87	2720	W I	0.365	3.45	$5d^5(^6S)6s \ ^7S_3$	$5d^5(^6S)6p \ ^7P_4$
5	407.43	2142	W I	0.365	3.40	$5d^5(^6S)6s \ ^7S_3$	$5d^5(^6S)6p \ ^7P_3$
6	422.77	1618	N II	21.59	24.53	$2s^2p^3p \ ^1D_2$	$2s^2p^4s \ ^1P_1$
7	444.70	1984	N II	20.40	23.19	$2s^2p^3p \ ^1P_1$	$2s^2p^3d \ ^1D_2$
8	463.05	3307	N II	18.48	21.15	$2s^2p^3s \ ^3P_2$	$2s^2p^3p \ ^3P_2$
9	480.32	1612	N II	20.66	23.24	$2s^2p^3p \ ^3D_3$	$2s^2p^3d \ ^3D_3$
10	489.51	1553	N II	17.87	20.40	$2s^2p^3 \ ^1D_2$	$2s^2p^3p \ ^1P_1$
11	500.51	7638	N II	20.66	23.14	$2s^2p^3p \ ^3D_3$	$2s^2p^3d \ ^3F_4$
12	520.16	2706	N I	11.60	13.98	$2s^2p^2(^3P)3p \ ^2S_{1/2}$	$2s^2p^2(^3P)5d \ ^2P_{3/2}$
13	567.95	3890	N II	18.48	20.66	$2s^2p^3s \ ^3P_2$	$2s^2p^3p \ ^3D_3$
14	594.16	2195	N II	21.15	23.24	$2s^2p^3p \ ^3P_2$	$2s^2p^3d \ ^3D_3$
15	656.27	2179	H $\alpha$	10.20	12.09	$2p \ ^2P_{1/2}^0$	$3d \ ^2D_{3/2}$
16	746.83	1535	N I	10.33	11.99	$2s^2p^2(^3P) 3s \ ^4P_{5/2}$	$2s^2p^2(^3P) 3p \ ^4S_{3/2}^o$
17	777.19	2838	O I	9.14	10.74	$2s^2p^3(^4S^o)3s \ ^5S_2$	$2s^2p^3(^4S^o)3p \ ^5P_3$
18	821.63	2166	N I	10.33	11.84	$2s^2p^2(^3P) 3s \ ^4P_{5/2}$	$2s^2p^2(^3P) 3p \ ^4P_{5/2}^o$
19	844.63	1363	O I	9.52	10.98	$2s^2p^3(^4S^o)3s \ ^3S_1$	$2s^2p^3(^4S^o)3p \ ^3P_2$
20	868.02	1512	N I	10.32	11.75	$2s^2p^2(^3P) 3s \ ^4P_{1/2}$	$2s^2p^2(^3P) 3p \ ^4D_{3/2}^o$
21	926.60	759	O I	10.74	12.07	$2s^2p^3(^4S^o)3p \ ^5P_3$	$2s^2p^3(^4S^o)3d \ ^5D_4^o$
22	1002.32	667	N II	26.21	27.45	$2s^2p^2(^3P)3p \ ^4D_{5/2}^o$	$2s^2p^2(^3P)3d \ ^2F_{5/2}$

synthesized in the plasma based on tungsten and air. The identification of Raman scattering spectra was conducted using references [17,18]. The majority of synthesized islands had characteristic dimensions of  $3 \times 3 \mu\text{m}$  and appeared dark in color in the images. Their Raman spectrum is shown in Figure 3.

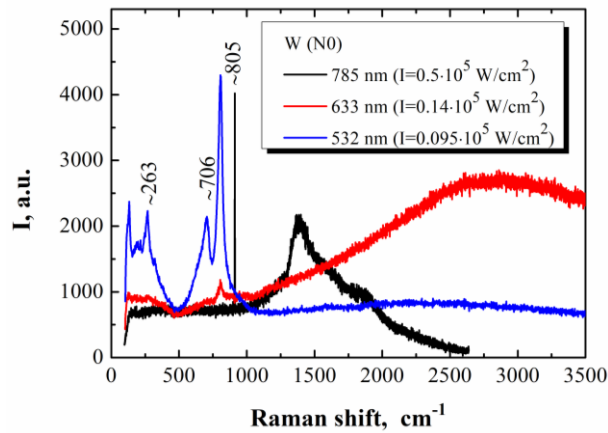


**Fig. 3.** Raman scattering spectrum of laser radiation from the island-like film deposited from the plasma of the mixture of air and tungsten vapors.

The bands observed in Figure 3 were reported in [17]. The band at a wavelength of  $\lambda = 263 \text{ cm}^{-1}$  corresponds to the O-W-O bond bending (W-O-W stretching modes) associated with oxygen bonding. The bands at  $\lambda = 706$  and  $805 \text{ cm}^{-1}$  belong to W-O stretching vibrations. The peaks of scattered light at wavelengths  $\lambda = 706$  and  $805 \text{ cm}^{-1}$  are associated with symmetric and asymmetric vibrations of the  $\text{W}^{6+}$ -O bonds (stretching modes) in the octahedral  $\text{WO}_6$  block [18]. The shifts of the peak maxima of the bands from the maxima reported in other authors' works are due to the associated formation of the  $\text{WO}_{3-x}$  structure through the creation of oxygen vacancies [18].

## Conclusions

Thus, it has been established that at atmospheric pressure between tungsten electrodes and at an

interelectrode distance of 2 mm, a uniform HVND ignited with a maximum voltage amplitude of up to 30 kV and a current of up to 100 A at  $P(\text{Air}) = 101 \text{ kPa}$ . The discharge ignited and existed in the form of bursts of individual half-waves lasting approximately 100 ns with almost constant amplitude for bursts lasting within 500 ns, which is optimal for electrode surface destruction and thin film synthesis from such plasma. The maximum pulse power of the HVND was 3.0 MW, and the highest energy in a single electrical pulse reached 312.6 mJ. Decreasing the air pressure from 101 to 13.3 kPa led to a significant reduction in the discharge's energy characteristics.

Investigation of the spectral characteristics of the HVND plasma in the gas-vapor mixtures "Air-W" showed that the most intense spectral lines were those of nitrogen atoms and ions; reducing the pulse current frequency from 1000 to 80 Hz led to a significant decrease in the intensity of all spectral lines and the continuum.

Analysis of the Raman scattering spectra of light from the films deposited from the discharge plasma showed that these were tungsten oxide ( $\text{WO}_3$ ) films.

**Shuaibov O.K.** – Doctor of Physical and Mathematical Sciences, Professor of the Department of Applied Physics and Quantum Electronics, Uzhhorod National University;  
**Hrytsak R.V.** – Ph.D., Senior Researcher, Associate Professor of the Department of Applied Physics and Quantum Electronics, Uzhhorod National University;  
**Minya O.Y.** – Ph.D., Senior Researcher, Senior Research Scientist of the Department of Applied Physics and Quantum Electronics, Uzhhorod National University;  
**Malinina A.O.** – Ph.D., Senior Researcher, Senior Research Scientist of the Department of Applied Physics and Quantum Electronics, Uzhhorod National University;  
**Shevera I.V.** – Senior Lecturer of the Department of Applied Physics and Quantum Electronics, Uzhhorod National University;  
**Bilak Y.Y.** – Ph.D., Associate Professor, Head of the Department of Systems Software, Faculty of Information Technology, Uzhhorod National University;  
**Homoki Z.T.** – Junior Researcher of the Department of Applied Physics and Quantum Electronics, Uzhhorod National University.

- [1] O.K. Shuaibov, A.O. Malinina, *Overstressed Nanosecond Discharge in the Gases at Atmospheric Pressure and Its Application for the Synthesis of Nanostructures Based on Transition Metals*, Progress in Physics of Metals, 22(3), 382(2021); <https://doi.org/10.15407/ufm.22.03.382>.
- [2] M.I. Vatralla, O.K. Shuaibov, O.Y. Mynya, R.V. Hrytsak, Z.T. Homoki 30th Anniversary Conference of the Institute of Electronic Physics of the National Academy of Sciences of Ukraine (Uzhhorod, Ukraine, 2022), p. 128.
- [3] G.A. Mesyats, *Ecton – Electron Avalanche from metal*, Phys.-Usp., 38(6), 567 (1995); <https://doi.org/10.1070/pu1995v038n06abeh000089>.
- [4] V.F. Tarasenko, *Runaway electrons preionized diffuse discharge* (New York, Nova Science Publishers Inc., 2014).
- [5] T.E. Itina, A.Voloshko, *Nanoparticle formation by laser ablation in air and by spark discharge at atmospheric pressure*, Appl. Phys. B, 113(3), 473(2013); <https://doi.org/10.5772/61303>.
- [6] Y. Shi, Y. Zang, *Designed growth of  $\text{WO}_3/\text{PEDOT}$  core/shell hybrid nanorod arrays with modulated electrochromic properties*, Chemical Engineering Journal, 335, 942 (2019); <https://doi.org/10.1016/j.cej.2018.08.163>.
- [7] Yu.O. Adamchuk, S.V. Chushchak, L.Z. Boguslavskii, A.V. Sinchuk *The Regularities of Titanium and Tungsten Carbide Formation from Products of Electric Explosion Destruction of Conductors*, Surface Engineering and Applied Electrochemistry, 59(3), 281(2023); <https://doi.org/10.3103/S1068375523030043>.

- [8] S.M. Karadeniz, *Novel Synthesis of Good Electrochromic Performance WO<sub>3</sub> Nanoplates Grown on Seeded FTO*, European Journal of Science and Technology, 27, 718(2021); <https://doi.org/10.31590/ejosat>.
- [9] Y.Zhen, B. Petter Jelle, T. Gao, *Electrochromic properties of WO<sub>3</sub> thin films: The role of film thickness*, Analytical Science Advances, 1, 124(2020); <https://doi.org/10.1002/ansa.202000072>.
- [10] R.J. Sáenz-Hernández, G.M. Herrera-Pérez, J.S. Uribe-Chavira, M. C. Grijalva-Castillo, J.T. Elizalde-Galindo, J. A. Matutes-Aquino, *Correlation between Thickness and Optical Properties in Nanocrystalline  $\gamma$ -Monoclinic WO<sub>3</sub> Thin Films*, Coatings, 12(11), 1727(2022); <https://doi.org/10.3390/coatings12111727>.
- [11] R. Shuker, Y. Binur, A. Szoke, *Studies of afterglows in noble-gas mixtures. A model for energy transfer in He/Xe*, Phys. Rev.A., 12(2), 515(1975); <https://doi.org/10.1103/PhysRevA.12.515>.
- [12] A. R. Striganov, Tables of spectral lines of neutral and ionized atoms (New York: Springer New York: 1968).
- [13] NIST Atomic Spectra Database Lines Form [https://physics.nist.gov/PhysRefData/ASD/lines\\_form.html](https://physics.nist.gov/PhysRefData/ASD/lines_form.html).
- [14] D.Z. Pai, D.L. Lacoste, C.O. Laux, *Nanosecond repetitively pulsed discharge in air at atmospheric pressure – the sparc regime*, Plasma Sources Sci. Technol., 19, 065015(2010); <https://doi.org/10.1088/0963-0252/19/6/065015>.
- [15] R.V. Hrytsak, O.Y. Minya, O.K. Shuaibov, Z.T. Homoki, M.I. Vatrana, Proceedings of the 1st International Scientific and Practical Internet Conference “Towards a Holistic Understanding: Interdisciplinary Approaches to Overcoming Global Challenges and Promoting Innovative Solutions” (Dnipro, Ukraine, 2024), p. 101.
- [16] O.K. Shuaibov, O.Y. Minya, Z.T. Homoki, I.V. Shevera, V.V. Danylo, *Method for Synthesizing Zinc Oxide Nanostructures with Automatic Ultraviolet Radiation Assistance*, Patent 124311, Ukraine, MPK (2021.01): C01G 9/02, No. a 2019 02824; Publ. 25.08.2021, Bulletin No.34, 6 p.
- [17] T. Sarmah, N. Aomoa, G. Bhattacharjee, S. Sarma, B. Bora, D.N. Srivastava, H. Bhuyan, M. Kakati, G. De Temmerman, *Plasma expansion synthesis of tungsten nanopowder*, Journal of Alloys and Compounds, 725, 606(2017); <https://doi.org/10.1016/j.jallcom.2017.07.207>.
- [18] F. Fang, J. Kennedy, J. Futter, T. Hopf, A. Markwitz, E. Manikandan, G. Henshaw, *Size-controlled synthesis and gas sensing application of tungsten oxide nanostructures produced by arc discharge*, Nanotechnology, 22(33), 335702 (2011); <https://doi.org/10.1088/0957-4484/22/33/335702>.

О.К. Шуаїбов, Р.В. Грицак, О.Й. Миня, А.О. Малініна, І.В. Шевера, Ю.Ю. Білак,  
З.Т. Гомокі

## Умови імпульсного газорозрядного синтезу тонких плівок оксиду вольфраму з плазми на суміші повітря з парами вольфраму

ДВНЗ «Ужгородський національний університет», Ужгород, Україна, [alexander.shuaibov@uzhnu.edu.ua](mailto:alexander.shuaibov@uzhnu.edu.ua)

Наведено характеристики високовольтного наносекундного розряду в газопарових сумішах «Air – W» при тисках повітря  $p = 101; 13.3$  кПа. Розряд запалювався між електродами з вольфраму. Утворення кластерів оксиду вольфраму в плазмі відбувалось в процесі внесення парів вольфраму в розрядний проміжок за екстонним механізмом, що створювало передумови для синтезу тонких плівок оксиду вольфраму (WO<sub>3</sub>), які осаджувались на скляній підкладці.

Досліджені оптичні властивості розряду з центральної області проміжку завширшки 2 мм. Виявлено основні компоненти, що викликають збудження у плазмі парогазової суміші на основі вольфраму і повітря. Дослідження спектрів раманівського розсіювання лазерного випромінювання синтезованими в експерименті тонкими плівками показало, що це острівкові плівки оксиду вольфраму (WO<sub>3</sub>).

**Ключові слова:** перенапружений наносекундний розряд, вольфрам, повітря, тонкі плівки, спектр випромінювання, плазма.